The electronic effect in the ⟨100⟩ edge dislocation core system with a carbon atom in α-iron: a first-principles study

2001 J. Phys.: Condens. Matter 13 4267

(http://iopscience.iop.org/0953-8984/13/19/307)

INSTITUTE OF PHYSICS PUBLISHING JOURNAL OF PHYSICS: CONDENSED MATTER

J. Phys.: Condens. Matter **13** (2001) 4267–4276 www.iop.org/Journals/cm PII: S0953-8984(01)20612-2

The electronic effect in the ⟨100⟩ edge dislocation core system with a carbon atom in α-iron: a first-principles study

Yuan Niu[1], **Shan-Ying Wang**[2], **Dong-Liang Zhao**[1] and **Chong-Yu Wang**[1,2,3]

[1] Central Iron and Steel Research Institute, Beijing 100081, China
[2] Department of Physics, Tsinghua University, Beijing 100084, China
[3] International Centre for Materials Physics, Academia Sinica, Shenyang 110016, China

Received 8 January 2001, in final form 16 March 2001

Abstract

Using the DMol molecular cluster method and the self-consistent discrete variational method based on density functional theory, we investigated the electronic effect in the ⟨100⟩ edge dislocation core system with a C atom in α-iron. A cluster model containing 96 atoms was used to simulate the local environment of the Fe edge dislocation, and the optimization results show that the C atom moves away from the compression side to the dilated region and falls into a flat tetrahedral interstice composed of four adjacent Fe atoms. We present the characteristic parameters including the structural energy, the interatomic energy, the partial density of states and the charge-density difference of the dislocation core system. The results suggest that the C atom stays steadily at a favourable site in the tetrahedron and forms strong covalent-like bonds with its adjacent Fe atoms. Moreover, the remarkable charge redistribution and the large binding energy drop in the dislocation core system indicate the formation of a C impurity–Fe edge dislocation complex which implies an effect of trapping of the dislocation core on the C atom.

1. Introduction

Dislocation, an important structural defect widely present in materials, has strong interactions with other defects such as impurity. The interactions greatly affect the mechanical properties of the material; one of these is described as an effect of trapping of a dislocation core on an impurity. The mechanical behaviours of dislocation are well described by the long-range elastic strain field derived from classical continuum theory, which can in most cases provide reliable answers to many mechanical problems. The success of the linear continuum elasticity theory is attributed to the fact that it smooths out the discrete lattice structure and allows a dislocation effect showing no structure dependence. But in the dislocation centre, which is surrounded by a region known as the dislocation core (DC), the theory ceases to be valid because of the presence of continuum singularity [1]. The radius of an effective DC region is

only about 1.25–1.65 Burgers vectors [2], and in such a small and local region, the discrete nature of the lattice structure becomes more important. Furthermore, the electronic effect may turn into a dominant factor. At present, one must resort to more appropriate theories—for example, the quantum theory—to obtain an accurate understanding of the interactions between the DC and impurities.

To our knowledge, there have been few experimental investigations at either the atomic level or the electronic level on DC in structural materials up to now. Nevertheless, theoretical efforts have been devoted to exploring DC problems by means of atomistic simulation and some semi-empirical electronic structure methods [3–10]. Vitek and Kubin [11, 12] reviewed separately a large number of the earlier studies on DC in close-packed metals in detail. It can be seen that using just a simple centre interaction potential such as the Morse potential in the studies, much fresh insight was obtained into stacking faults, the behaviour of dislocation dissociation, and the atomic structure of the DC and the properties of screw and non-screw dislocations. De Hosson [13] investigated the localized states of an edge dislocation in α-iron by the self-consistent-field X_α method with a multiple-scattering model, and determined the changes in electronic structure of the lattice near the core region of the defect in α-iron. He found that the variations of hydrostatic pressure arising from an edge dislocation can produce a rearrangement of the conduction electrons of the Fe atom, and electrons tend to flow away from the compression side toward the dilated region. Using a tight-binding-type electronic theory, Masuda *et al* [14] studied the atomic structures and calculated the energies of DC of $1/2\langle 111\rangle\{110\}$ and $1/2\langle 111\rangle\{112\}$ edge dislocations in a bcc transition metal. They showed that the electronic effect on the dislocation core is important and the Peierls stress of the screw dislocation is approximately ten times larger than that of the edge dislocation. More recently, by use of semi-empirical atom superposition and electron delocalization molecular orbital theory, Gesari *et al* [15] studied the interaction of hydrogen with α-iron. They simulated the adsorptions of hydrogen on $(\bar{1}12)$ and (110) planes and those in an edge dislocation. They found that the H–Fe interaction is stronger near the centre of the dislocation.

In recent years, density functional theory [16, 17] as well as the various subsequently developed first-principles methods have shown great potential and advantages as regards aspects of treating low dimensions or defect systems [18]. Since studies on DC and DC with impurities are of great importance, we have performed careful and intensive calculations by means of the first-principles methods on the electronic structure and energy of DC and DC with light impurities including B, C, N, O, P, and S for edge dislocations in α-iron. This enables us to understand well the interactions between the DC and impurities. In this paper, we will report only the results for the DC with a single carbon impurity (called the carbon DC). The results for other impurities are in preparation.

2. Theoretical method and computational details

In the present study, we employed two widely used first-principles methods: the DMol method [19,20] and the discrete variational method (DVM) [21,22] based on density functional theory. As is well known, the cluster model is a convenient basis for studying electronic properties that are primarily functions of the local environment of the defect system. The two methods, in which the molecular orbitals are expressed as linear combinations of atomic orbitals, enable us to use the cluster model to study a real system without substantially increasing the computational time requirement. The DMol method is capable of calculating the energy gradient for each atom. The equilibrium atomic configuration and the total energy corresponding to the ground state can be obtained when the forces on the relaxed atoms become sufficiently small. We also made use of the DVM to determine the charge-density distribution,

partial density of states (PDOS), eigenvalues, and other relevant physical parameters of the system in the ground state.

In order to get an atomic configuration of an edge dislocation core for the first-principles calculation, we first adopt the molecular dynamics (MD) method with the Finnis–Sinclair potential [23, 24], a well known semi-empirical N-body potential for transition metals, to simulate a ⟨100⟩ edge dislocation in α-iron. The initial atomic configuration of the dislocation system for the MD simulation was determined using elastic displacement-field theory. The Burgers vector is $a_0[100]$ (a_0 is the lattice constant of α-iron). The dislocation line is along the [001] direction and the slip plane is (010). After a full relaxation under periodic conditions along the [001] direction and fixed boundary conditions along the [010] and [100] directions, we got an atomic configuration with C_{2v} symmetry for the ⟨100⟩ edge dislocation system, which is quite similar to the result obtained by Gehlen *et al* [2]. Then, for the first-principles calculation, we constructed a cluster model of DC from the MD results (called the initial DC), which consists of 96 Fe atoms as illustrated in figure 1. The cluster model contains five layers with a stacking sequence ABABA along the [001] direction. An interstice enclosed by eight Fe atoms labelled Fe1 to Fe8 can be found in the initial DC system. A carbon atom is introduced into the interstice for the purpose of studying the electronic effect of the DC with impurity. It can be expected that the C atom will induce a local distortion of the surrounding Fe atom sites because of the C–Fe interaction. In view of that, the smallest distance between Fe and C is the key factor in evaluating their interactions; only the C atom and its neighbouring Fe1 to Fe8 atoms are allowed to relax according to forces in the DMol calculation. We obtained an optimized geometry structure located at a local energy minimum within the tolerances of

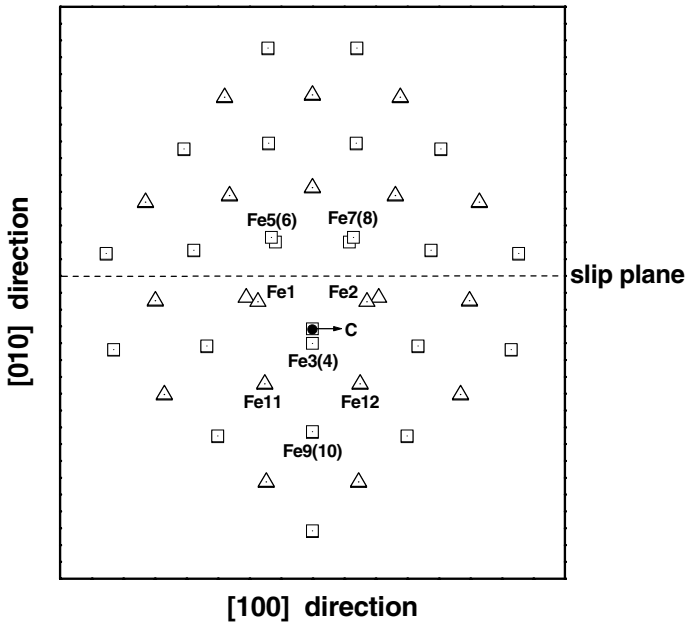

Figure 1. The atomic configurations in the initial DC system and the carbon DC system. The triangular and square symbols denote the Fe atoms on stacking planes A and B respectively along the dislocation line direction, i.e. the [001] direction. The symbols with and without the central dot denote the Fe atoms in the carbon DC system and the initial DC system respectively. The C atom is symbolized by a solid circle. The dashed line is a guide to allow a clear visualization of the slip plane (010). One can see clearly that Fe1 to Fe8 atoms shift away upon DMol relaxation.

0.001 eV and 0.0005 Å for the energy gradient and atomic displacement respectively. In the DMol calculation, the double numerical polarized bases as well as the Vosko–Wilk–Nusair local exchange–correlation functional [25] with the Becke–Perdew–Wang general gradient approximation correction [26,27] are used in order to produce more reliable results. Using the atomic coordinates taken from the DMol relaxation calculation, we investigated the electronic structure by means of the DVM. The funnel potential [28] is added in the basis to induce the bond states. The Coulomb potential is calculated in a self-consistent charge approximation and the Vosko–Wilk–Nusair exchange–correlation potential is employed. About 1000 integration points per atom are used in the computation.

3. Features of the local atomic configuration

Clearly, long-range MD relaxation is sometimes insufficient in dealing with the problem of a local system. One may need to properly take the local atomic relaxation into account by use of the first-principles method. In order to avoid the possible inadequacy of the MD relaxation and to clarify the significance of the local lattice deformation induced by impurity, we performed a total-energy calculation on the initial DC system as well as a relaxation calculation on the initial DC system (called the 'clean DC system after relaxation') similar to that on the carbon DC system. The main results for the three systems are summarized in table 1. Let us discuss the initial DC system and the clean DC system first. We can see a remarkable modification of the interatomic distance in the initial DC system produced by DMol relaxation. Comparing with the MD results, DMol relaxation gave an increasing interatomic distance in the section above the slip plane (010) and a decreasing interatomic distance below the slip plane. In the stacking layers A and B, the distance between the Fe1 and Fe2 atoms (denoted by $d_{\mathrm{Fe1-Fe2}}$) reduces by 11.4% and $d_{\mathrm{Fe5-Fe7}}$ expands by 11.1%, while $d_{\mathrm{Fe3-Fe9}}$ is almost unchanged. Along the direction of the dislocation line, $d_{\mathrm{Fe3-Fe4}}$ reduces by 11.2% and $d_{\mathrm{Fe5-Fe6}}$ expands by 11.2%. The difference in binding energy (defined as the difference in total energy between the bonding-atom system and the free-atom system) between the initial DC system and the clean DC system is small, only 0.92 eV. It appears that for the edge dislocation system, the correction from the first-principles relaxation calculation to the atomic bond length may surpass that to the energy, but both corrections are essential. Similar results were found in the studies on iron grain boundaries by Tang and Freeman [29]. We now turn to the carbon DC system. Comparing with the clean DC system, $d_{\mathrm{Fe1-Fe2}}$ in the carbon DC system reduces by 0.27 Å, while $d_{\mathrm{Fe5-Fe6}}$ and $d_{\mathrm{Fe5-Fe7}}$ change little, by only -0.04 Å and 0.01 Å. In order of size, the interatomic distances for the selected Fe–C atomic pairs are as follows: $d_{\mathrm{C-Fe3}}$ is 1.84 Å, $d_{\mathrm{C-Fe1}}$ is 1.92 Å, $d_{\mathrm{C-Fe11}}$ is 2.21 Å, $d_{\mathrm{C-Fe9}}$ is 3.36 Å, and $d_{\mathrm{C-Fe5}}$ is 3.43 Å. It is very interesting that when entering

Table 1. The calculated interatomic distances (in Å) of the selected atomic pairs in the initial DC system, the clean DC system, and the carbon DC system, and the binding energies E_b (in eV) of the three systems.

	Initial DC	Clean DC	Carbon DC
$d_{\mathrm{Fe1-Fe2}}$	4.20	3.72	3.45
$d_{\mathrm{Fe3-Fe4}}$	2.87	2.55	3.60
$d_{\mathrm{Fe5-Fe6}}$	2.87	3.19	3.23
$d_{\mathrm{Fe5-Fe7}}$	2.35	2.61	2.60
$d_{\mathrm{Fe3-Fe9}}$	3.08	3.10	2.65
E_b	−433.98	−434.90	−445.05

into the interstice, the C atom has a strong tendency to move away from the compression side into the dilated region. As a result, the Fe3 and Fe4 atoms are pushed down by the C impurity along the [010] direction by about 0.45 Å, and the distance between them increases notably, by about 1.05 Å. The C atom falls eventually into a flat tetrahedral interstice formed by Fe1 to Fe4 atoms. The binding energy of the carbon DC system is 10.15 eV lower than that of the clean DC system, which shows that the carbon DC system is more stable. The analyses indicate that a C impurity could induce the obvious variation of its local environment in the iron DC system.

4. Interatomic interactions

In order to study the interaction between the two atoms in the carbon DC system, we calculated two characteristic quantities: the structural energy in the real-space Green function method and the interatomic energy [30, 31]. The structural energy is expressed as

$$E_l = \int_{-\infty}^{E_F} n_l(E) E \, \mathrm{d}E$$

where $n_l(E)$ is the local density of states of atom l, and E_F is the Fermi energy of the system. It was used to define the impurity formation energy in treating the defect system [32]. An impurity at its stable atomic site usually displays a low structural energy. The interatomic energy E_{lm} for atoms l and m is defined by

$$E_{lm} = \sum_{\sigma} \sum_{n} \sum_{\alpha\beta} N_n^{\sigma} a_{n\alpha l}^{*\sigma} a_{n\beta m}^{\sigma} H_{\beta m \alpha l}^{\sigma}$$

where N_n^{σ} is the occupation number for the molecular orbital ψ_n^{σ} with the spin state σ, $a_{n\alpha l}^{\sigma} = \langle \phi_{\alpha l} | \psi_n^{\sigma} \rangle$, and $H_{\beta m \alpha l}^{\sigma}$ is the Hamiltonian matrix element connecting the atomic orbital ϕ_{β} of atom m to the atomic orbital ϕ_{α} of atom l. The interatomic energy can provide a good estimate of the bonding capability of two atoms as the usual bond order parameter. However, it contains more physics because it relates to the Hamiltonian. Usually, a minus number with larger absolute value means a stronger interaction between the two atoms. Such a parameter was successfully utilized in studies on Ni_3Al grain boundary problems [30, 31]. In this work, the structural energy and interatomic energy are calculated using the data obtained by the DVM.

The structural energies of some interesting sites are listed in table 2. Compared with those in the clean DC system, Fe atoms in the carbon DC system show small changes of structural energy except for the Fe11 atom. The changes can be attributed mainly to the C–Fe interactions. In the carbon DC system, the C atom has the lowest structural energy, about −7.41 eV. The unexpectedly low structural energy indicates that the C atom is firmly caught by the DC, which implies an effect of trapping of the DC on the impurity.

Table 2. The calculated structural energies (in eV) of the selected atomic sites in the clean DC system and the carbon DC system.

	Clean DC	Carbon DC
C site	—	−7.41
Fe1 site	−2.86	−2.80
Fe3 site	−2.61	−2.72
Fe5 site	−2.88	−2.95
Fe9 site	−2.59	−2.68
Fe11 site	−2.77	−2.78

Table 3 presents the interatomic energies for some typical atomic pairs (most of the selected atomic pairs consist of two atoms with a nearest-neighbouring relationship). We can see that in the carbon DC system, the strength of the bonding between the host Fe atoms which are close to the C atom is weakened. The interatomic energies of the Fe1–Fe3 and Fe3–Fe4 atomic pairs show changes larger than 1.76 eV, and those of Fe3–Fe5 and Fe3–Fe11 atomic pairs show changes close to half of the previous value, about 0.69 eV, while the C atom hardly affects the interactions between the Fe atoms at a larger distance from it. For example, the changes of interatomic energy are only 0.11 eV and −0.01 eV for Fe5–Fe6 and Fe5–Fe7 atomic pairs respectively. It should be noted that C–Fe1 and C–Fe3 atomic pairs display interatomic energies much lower than −3.45 eV, but C–Fe5 and C–Fe11 atomic pairs display values of 0.03 eV and −1.20 eV respectively. From these results, we conclude that in the carbon DC system, C impurity could weaken the interactions between the adjacent host Fe atoms, and a C atom could have strong interactions and form strong bonds with the adjacent host Fe atoms.

Table 3. The calculated interatomic energies (in eV) of the selected atomic pairs in the clean DC system and the carbon DC system.

	Clean DC	Carbon DC
Fe1–Fe3	−2.39	−0.37
Fe3–Fe4	−1.73	0.03
Fe3–Fe5	−1.08	−0.39
Fe3–Fe11	−1.39	−0.64
Fe5–Fe6	−0.51	−0.40
Fe5–Fe7	−1.99	−2.00
C–Fe1	—	−3.45
C–Fe3	—	−3.65
C–Fe5	—	0.03
C–Fe11	—	−1.20

5. Charge distribution and magnetism

For a defect system such as a DC, the charge redistribution and the charge transfer between the impurity and its surrounding host atoms would significantly affect the interatomic bonding. Table 4 lists the electron occupation number and the magnetic moment in the valence orbital obtained by Mulliken population analysis [33] for the C atom and its neighbouring Fe atoms. We found that the C atom obtains 0.68 electrons from the adjacent Fe atoms, which are mainly assigned to its 2p orbital. The adjacent Fe1, Fe3, and Fe11 atoms lost electrons: about $0.23e$, $0.21e$, and $0.14e$ respectively, and most of them are from the 4s and 4p orbitals and are transferred to the C atom, which implies C 2s, 2p–Fe 4s, 4p hybridizations. The results of charge transfers from the Fe atoms to the C atom are consistent with the Pauling electronegativity values (C: 2.6; Fe: 1.83); that is, C has much stronger ability to obtain electrons than Fe.

It is well known that the exchange interaction, which is sensitive to the configuration of metal atoms, is a key factor in determining the low-temperature magnetism of α-iron. We can see that in the complicated local environment in the DC system, Fe atoms show magnetism very different from that in the perfect system. For the clean DC system, the magnetic moments of Fe1 and Fe3 atoms are decreased remarkably compared to that of perfect α-iron (about 2.20 μ_B per atom), and form an antiferromagnetic state with those of other host Fe atoms. By contrast, in the carbon DC system, because of the strong orbital hybridization between the Fe

Table 4. The electron occupation numbers N_0 (N) and their sum Q, and the magnetic moments S_0 (S) (in μ_B) and their sum M for each atom in the clean DC system (carbon DC system). For the Fe atom, $\Delta N = N - N_0$, $\Delta Q = Q$(carbon DC) $- Q$(clean DC). For the C atom, ΔQ is defined as the difference from that of the free atom.

		Clean DC		Carbon DC			
		N_0	S_0	N	S	ΔN	ΔQ
C	2s			1.51	−0.05		
	2p			3.18	−0.30		
	Q, M			4.68	−0.35		+0.68
Fe1	4s	0.79	−0.04	0.68	0.04	−0.11	
	4p	0.88	−0.13	0.75	0.01	−0.13	
	3d	6.32	−1.57	6.33	2.10	+0.01	
	Q, M	7.98	−1.74	7.75	2.16		−0.23
Fe3	4s	0.79	−0.05	0.65	−0.06	−0.14	
	4p	0.89	−0.16	0.80	−0.14	−0.09	
	3d	6.34	−0.88	6.36	1.33	+0.02	
	Q, M	8.02	−1.08	7.81	1.13		−0.21
Fe11	4s	0.79	0.02	0.69	−0.01	−0.10	
	4p	0.82	−0.06	0.77	−0.10	−0.05	
	3d	6.33	2.18	6.34	2.40	+0.01	
	Q, M	7.94	2.13	7.80	2.29		−0.14

and C atoms, the magnetic moments of Fe1 and Fe3 atoms increase and flip over to favour a ferromagnetic state with those of the other host Fe atoms. Meanwhile, the 2s, 2p electrons of the C atom are spin polarized and the C atom exhibits a small magnetic moment, which is antiparallel to those of the host Fe atoms.

In figures 2 and 3, the PDOS curves for the Fe1 and Fe3 atoms in the clean DC system and those for the Fe1, Fe3, and C atoms in the carbon DC system are depicted respectively.

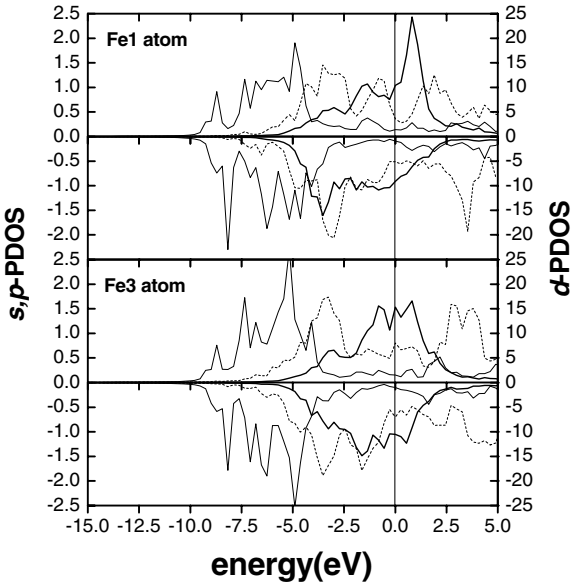

Figure 2. The atomic partial density of states (PDOS) in the clean DC system. The thick solid lines, thin solid lines, and dashed lines denote d, s, and p electronic states respectively. The PDOS for the spin-up state and spin-down state are shown in the upper panel and the lower panel respectively. The Fermi level is shifted to zero.

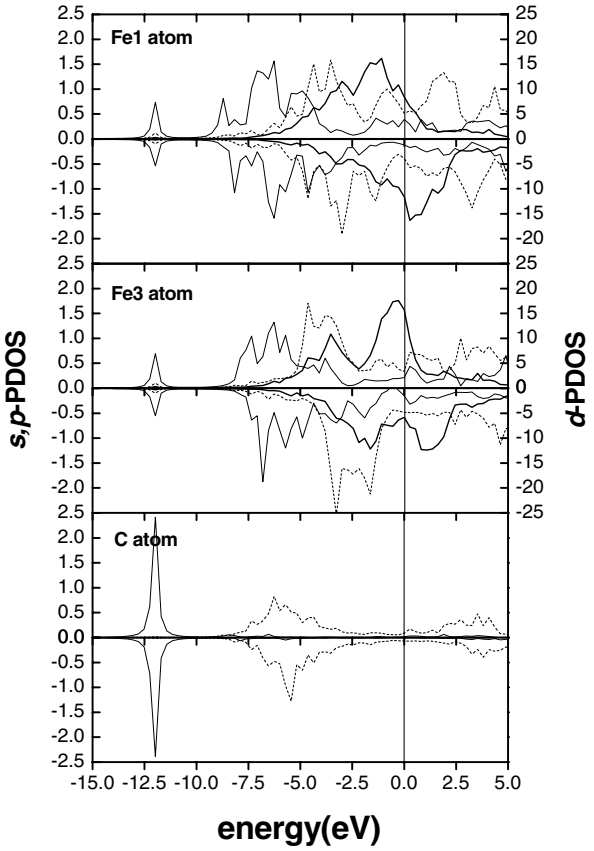

Figure 3. The atomic partial density of states (PDOS) in the carbon DC system. The thick solid lines, thin solid lines, and dashed lines denote d, s, and p electronic states respectively. The PDOS for the spin-up state and spin-down state are shown in the upper panel and the lower panel respectively. The Fermi level is shifted to zero.

The large exchange splitting of the Fe 3d orbital and the weakly spin-polarized Fe 4s, 4p orbitals can be seen clearly. The PDOS of adjacent Fe1 and Fe3 atoms in clean DC show two main hybridization features—namely strong hybridization of Fe 4p orbitals with Fe 3d orbitals, and weak hybridizations of the Fe 4s orbital with Fe 3d, 4s orbitals—which are different from the case for the perfect α-iron system. In contrast to those of the clean DC system, the PDOS features of the adjacent Fe atoms in the carbon DC system change a lot because of the charge transfer from the Fe atom to the C atom. From figure 3, we can see that a new remarkable resonant feature appears at a very low energy of about -12.0 eV, which implies strong hybridization of the C 2s orbital with Fe1 4s, Fe3 4s orbitals. A further strong hybridization of the C 2p orbital with Fe1 4s, Fe3 4s orbitals can also be found in the low-energy range from about -9.0 eV to -2.5 eV. The PDOS of the C atom distributed in the low-energy range accounts for its low structural energy in table 2. We can also find large modifications of the PDOS distributions of 4p, 3d orbitals of Fe1 and Fe3 atoms in figure 3.

From the charge density of the carbon DC, one can obtain a direct understanding of the interatomic bonding characteristics. The charge-density differences on the centre stacking plane A which contains C, Fe1, and Fe2 atoms, and a (010) plane which contains C, Fe3, and Fe4 atoms are plotted in figure 4. Here, the charge-density difference is defined as $\Delta\rho = \rho(\text{carbon DC}) - \rho(\text{initial DC}) - \rho_{\text{free}}(\text{C})$. The contour curves in figure 4 clearly show the charge redistribution in the carbon DC system. We can see that a lot of electrons accumulate in the vicinity of the C atom and some strong charge-correlation regions are formed between the C atom and its neighbouring Fe1 to Fe4 atoms. The characteristics of the charge

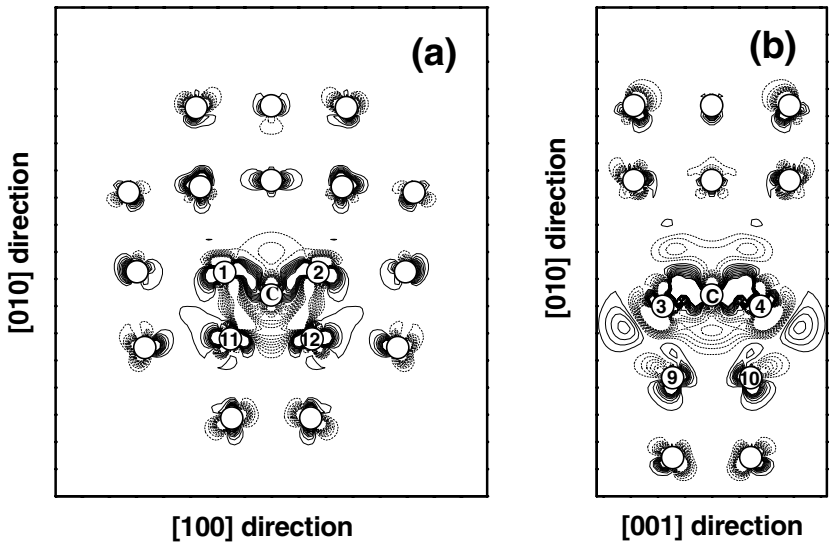

Figure 4. The charge-density difference for two planes: (a) the centre stacking plane A along the [001] direction containing C, Fe1, and Fe2 atoms; (b) a (100) plane containing C, Fe3, and Fe4 atoms. The circled numbers correspond to those in figure 1. The contour spacings are 0.001 e Å^{-3}. Solid lines and dashed lines indicate the gain and the loss of electrons respectively.

distribution indicate the strong interactions between the C atom and its adjacent Fe atoms as well as the covalent-like bonds formed therein. However, there are no evident charge-correlation regions—but lots of lost-electron regions can be found around the Fe11 to Fe12 atoms. These results agree well with the analyses of the interatomic energy and the atomic PDOS.

6. Conclusions

We have studied the electronic effect in the dislocation core system with the presence of a C atom in α-iron by means of first-principles methods. It is found that the C atom moves away from the compression side to the dilated region and falls into a flat tetrahedral interstice composed of four adjacent Fe atoms in the dilated region, and forms strong covalent-like bonds with the adjacent Fe atoms. There are charge transfers from Fe atoms to the C atom and strong hybridizations between the C 2s, 2p orbitals and the adjacent Fe 4s, 4p orbitals. These results suggest that a C atom could promote the formation of a carbon impurity–Fe edge dislocation complex, and subsequently the dislocation core could exert a trapping effect on the C impurity, which implies a quantum-mechanical effect nature of the Cottrell atmosphere in the dislocation system.

Acknowledgments

The authors are grateful to Dr Hongbo Liu for his helpful work in the MD simulation of the dislocation. This work was supported by the National Natural Science Foundation of China (59971041) and 973 National Pandeng Project (G2000067102).

References

[1] Eshelby J D 1956 *Solid State Physics* vol 3 (New York: Academic) p 79
[2] Gehlen P C, Rosenfield A R and Hahn G T 1968 *J. Appl. Phys.* **39** 5246
[3] Masuda K and Sato A 1978 *Phil. Mag.* B **37** 531
[4] Sato A and Masuda K 1981 *Phil. Mag.* B **43** 1
[5] Masuda K and Sato A 1981 *J. Phys. Soc. Japan* **50** 569
[6] Bacon D J and Martin J W 1981 *Phil. Mag.* A **43** 901
[7] Minonishi Y, Ishioka S, Koiwa M, Morozumi S and Yamaguchi M 1981 *Phil. Mag.* A **43** 1017
[8] Minonishi Y, Ishioka S, Koiwa M, Morozumi S and Yamaguchi M 1981 *Phil. Mag.* A **44** 1225
[9] Bacon D J and Liang M H 1986 *Phil. Mag.* A **53** 163
[10] Liang M H and Bacon D J 1986 *Phil. Mag.* A **53** 181
[11] Vitek V 1974 *Cryst. Latt. Defects* **5** 1
[12] Kubin L P 1982 *Rev. Defects Behav. Mater.* **1** 181
[13] De Hosson J Th M 1980 *Int. J. Quantum Chem.* **18** 575
[14] Masuda K, Kobayashi K, Sato A and Mori T 1981 *Phil. Mag.* B **43** 19
[15] Gesari S, Irigoyen B and Juan A 1998 *J. Phys. D: Appl. Phys.* **31** 2179
[16] Hohenberg P C and Kohn W 1964 *Phys. Rev.* **136** B864
[17] Kohn W and Sham L J 1965 *Phys. Rev.* **140** A1133
[18] Freeman A J 1995 *Annu. Rev. Mater. Sci.* **25** 7
[19] Delley B 1990 *J. Chem. Phys.* **92** 508
[20] Delley B 1991 *J. Chem. Phys.* **94** 7245
[21] Ellis D E and Painter G S 1970 *Phys. Rev.* B **2** 2887
[22] Delley B, Ellis D E, Freeman A J, Baerends E J and Post D 1983 *Phys. Rev.* B **27** 2132
[23] Finnis M W and Sinclair J E 1984 *Phil. Mag.* A **50** 45
[24] Finnis M W and Sinclair J E 1986 *Phil. Mag.* A **53** 161
[25] Vosko S J, Wilk L and Nusair M 1980 *Can. J. Phys.* **58** 1200
[26] Becke A D 1988 *Phys. Rev.* A **38** 3098
[27] Perdew P and Wang Y 1992 *Phys. Rev.* B **45** 13 244
[28] Averill F W and Ellis D E 1973 *J. Chem. Phys.* **59** 6412
[29] Tang S P and Freeman A J 1994 *Phys. Rev.* B **50** 1
[30] Wang F H and Wang C Y 1997 *J. Phys.: Condens. Matter* **9** 4499
[31] Wang F H and Wang C Y 1998 *Phys. Rev.* B **57** 289
[32] Wang C Y and Zhao D L 1994 *Mater. Res. Soc. Symp. Proc.* **571** 318
[33] Mulliken R S 1955 *J. Chem. Phys.* **23** 1833